



Reemergence of the collective mode in ^3He and electron layers

Helga M. Böhm, Robert Holler, Eckhard Krotscheck, Martin Panholzer, Henri Godfrin, Mathias Meschke, Hans-Jochen Lauter

► To cite this version:

Helga M. Böhm, Robert Holler, Eckhard Krotscheck, Martin Panholzer, Henri Godfrin, et al.. Reemergence of the collective mode in ^3He and electron layers. *International Journal of Modern Physics B*, 2010, 24 (25-26), pp.4889. 10.1142/S0217979210057079 . hal-00921240

HAL Id: hal-00921240

<https://hal.science/hal-00921240>

Submitted on 20 Dec 2013

HAL is a multi-disciplinary open access archive for the deposit and dissemination of scientific research documents, whether they are published or not. The documents may come from teaching and research institutions in France or abroad, or from public or private research centers.

L'archive ouverte pluridisciplinaire **HAL**, est destinée au dépôt et à la diffusion de documents scientifiques de niveau recherche, publiés ou non, émanant des établissements d'enseignement et de recherche français ou étrangers, des laboratoires publics ou privés.

International Journal of Modern Physics B
 © World Scientific Publishing Company

REEMERGENCE OF THE COLLECTIVE MODE IN ^3He AND ELECTRON LAYERS

Helga M. BÖHM, Robert HOLLER, Eckhard KROTSCHKE, Martin PANHOLZER
*Institute of Theoretical Physics, Johannes Kepler University, Altenbergerstr. 69
 A-4040 Linz, Austria*

Henri GODFRIN¹, Mathias MESCHKE¹, Hans-Jochen LAUTER²

¹*Institut Néel, CNRS et Université Joseph Fourier,
 Grenoble Cedex 9, BP 166, F-38042 France*

²*Institut Laue-Langevin,
 Grenoble Cedex 9, BP 156, F-38042 France*

Revised Day Month Year

Neutron scattering experiments on a ^3He layer on graphite show an unexpected behavior of the collective mode. After having been broadened by Landau damping at intermediate wave vectors, the phonon-roton mode resharpens at large wave vectors and even emerges from the particle-hole continuum at low energies. The measured spectra cannot be explained by a random phase approximation with any static interaction. We show here that the data are well described if dynamic two-pair fluctuations are accounted for. We predict similar effects for electron layers.

Keywords: Fermi liquids; ^3He ; electron liquid, neutron scattering, dynamic correlations.

1. Motivation

1.1. *An experimentum crucis*

Understanding the excitations of quantum fluids has been a major goal of condensed matter physics for decades. For the helium liquids, a prime example of strongly correlated systems, Pines¹ argued long ago that the phonon-maxon-roton mode in ^4He and ^3He has a common physical origin in their strong and identical interatomic interaction. Quantum statistics, though quantitatively relevant, plays a less important role for the general features of the collective mode. The long wavelength plasmon in an electron liquid,^{2,3} caused by a completely different interaction, is explained by the same theories that proved successful for the neutral systems.

There is, however, a fundamental difference in bosonic and fermionic spectra: whereas for bosons the collective mode remains well-defined over a wide range of wave vectors q , it is rapidly damped when it enters the domain of incoherent single-particle-hole (PH) excitations (“Landau damping”). Now our refined measurements

2 *H.M. Böhm, R. Holler, E. Krotscheck, M. Panholzer, H. Godfrin, M. Meschke, H.J. Lauter*

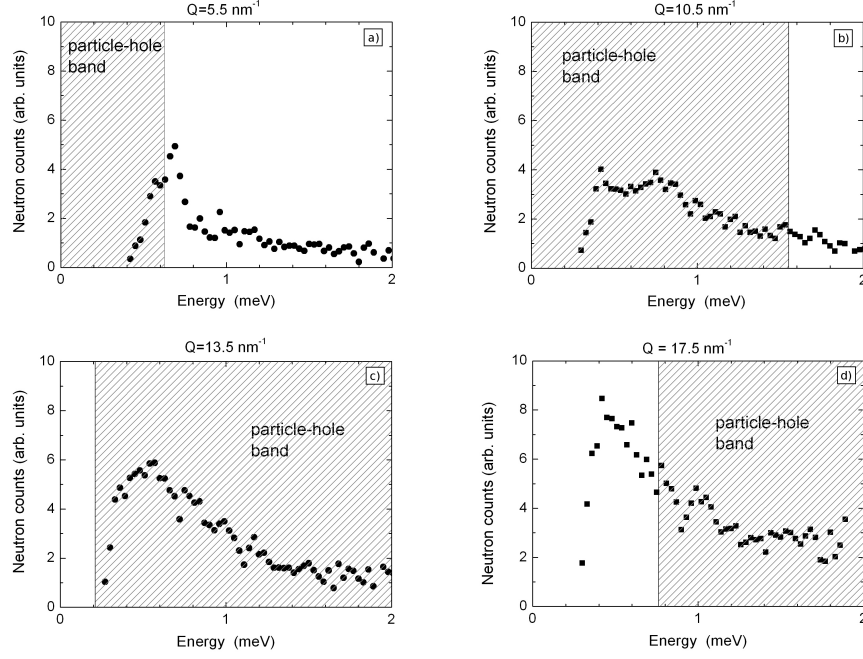


Fig. 1. Dynamic structure factor of two-dimensional ^3He , obtained from inelastic neutron scattering at 4 different wave vectors Q and an areal density of 4.9 nm^{-2} . The shaded area is the particle-hole continuum. Note the strong peak below it in the lower right figure.

reveal a pronounced excitation at atomic wave vectors (Fig. 1). At the Institut Laue-Langevin (ILL) we determined the dynamic structure factor $S(q, E)$ of a mono layer of liquid ^3He ($E = \hbar\omega$ is the excitation energy). It is clearly seen that the collective mode, sharp at small q and damped at intermediate q (Fig. 1 a) and b)), recollects strength (Fig. 1c) and even re-emerges at the lower end of the PH continuum (Fig. 1d).

1.2. *Effective static interactions*

These unexpected findings put the existing theories to a severe test. In the long wavelength limit the common paradigm of quasi-particle excitations^{2,4–5} works well. For the electron liquid it has led to the random phase approximation (RPA), which gives the density-density response function χ of a system as

$$\chi^{\text{RPA}} = \frac{\chi^0(q, \omega)}{1 - v(q)\chi^0(q, \omega)} \quad , \quad (1)$$

where χ^0 is the Lindhard function and $v(q)$ is the Fourier transform of the interaction. For many systems in nature (e.g. with hard-core or $1/r^3$ potentials) this transform does not exist. How the RPA can be extended to such strong interactions

was shown in Ref. 6; it amounts to replacing the bare $v(q)$ in (1) by an appropriately defined effective static interaction. Requiring consistency of $\Im m \chi$ and the static structure via the fluctuation-dissipation theorem unambiguously identifies this interaction as the “irreducible particle-hole interaction” $V_{\text{p-h}}$

$$\chi^{\text{cRPA}} = \frac{\chi^0(q, \omega)}{1 - V_{\text{p-h}}(q) \chi^0(q, \omega)} . \quad (2)$$

Different choices of static interactions (formulated via “local field corrections”) were presented for the electron liquid,^{3,7} based on different self-consistency requirements. None of these, however, can provide an excitation spectrum *qualitatively* different from a low q collective mode, vanishing into the PH continuum.

1.3. Effective mass

Before entering the PH continuum, measured collective modes visibly deviate from the (c)RPA predictions based on (2). A common cure^{8,9} is to introduce an effective mass m^* , replacing the bare m in the Lindhard function. Again, such an approach cannot give the newly observed re-emergent zero-sound mode. Furthermore, m^* in ^3He is strongly q -dependent with a peak around the Fermi vector k_F and additionally leads to a wrong density dependence of the mode.¹⁰ We do *not* claim that correcting for effective mass effects is unimportant. Rather we here concentrate on clarifying the physical reason for the sharpening of the collective mode at high q .

2. Theory: Overview

2.1. Ground state theory

For strongly interacting fermions the variational Jastrow–Feenberg¹¹ *ansatz* has highly successfully described most ground state properties:

$$|\Psi_{\text{GS}}\rangle \equiv |\Psi_0\rangle = \frac{1}{\sqrt{\mathcal{N}_{\text{GS}}}} e^{\frac{1}{2}\hat{U}} |\Phi_0\rangle . \quad (3)$$

Here, \mathcal{N}_{GS} is the normalization, Φ_0 a Slater determinant and \hat{U} contains, in principle, correlation functions of arbitrarily high order n

$$\hat{U} = \sum_i u^{(1)}(\mathbf{r}_i) + \sum_{i<j} u^{(2)}(\mathbf{r}_i, \mathbf{r}_j) + \sum_{i<j<k} u^{(3)}(\mathbf{r}_i, \mathbf{r}_j, \mathbf{r}_k) + \dots . \quad (4)$$

These functions are determined by *functionally minimizing* the ground state energy $E_{\text{GS}} \equiv H_{0,0}$, thus providing a parameter-free and robust ab-initio theory. The essential physics contained in Eq. (3) is to intuitively account for core exclusion; in systems like ^3He , where no Fourier transform of the interaction exists, $\exp\{u^{(n)}\}$ is well-behaved. For the practical evaluation of the energy expectation value, Fermi hypernetted chain (FHNC) theory has the advantage of being consistent with the optimization procedure at any order n , summing ladder diagrams exactly and rings in a local approximation. This way both, short as well as long range correlations are very well described.¹²

4 *H.M. Böhm, R. Holler, E. Krotscheck, M. Panholzer, H. Godfrin, M. Meschke, H.J. Lauter*

If necessary, the nodal surface problem inherent in Eq. (3) can be overcome by using correlated basis function (CBF) theory.^{11,12} Here the correlation operator

$$F_{\text{GS}} \equiv \exp\{\frac{1}{2}\hat{U}\} \quad (5)$$

is applied not to the ground state but to determinants describing free excitations

$$|\Psi_{\mathbf{m}}\rangle \equiv \frac{1}{\sqrt{N_{\mathbf{m}}}} F_{\text{GS}} |\Phi_{\mathbf{m}}\rangle . \quad (6)$$

This creates a complete set of non-orthogonal functions. Conventional basis functions, *e.g.* plane waves for uniform systems with hard cores, require infinite summations of large (often divergent) terms: by contrast, CBF incorporates important aspects of the correlations right from the starting point.

The matrix elements of unity and of the Hamiltonian \hat{H} in the basis (6)

$$\begin{aligned} M_{\mathbf{m},\mathbf{m}'} &\equiv \langle \Psi_{\mathbf{m}} | \Psi_{\mathbf{m}'} \rangle \equiv \delta_{\mathbf{m},\mathbf{m}'} + N_{\mathbf{m},\mathbf{m}'} \\ H_{\mathbf{m},\mathbf{m}'} &\equiv \langle \Psi_{\mathbf{m}} | \hat{H} | \Psi_{\mathbf{m}'} \rangle \equiv H'_{\mathbf{m},\mathbf{m}'} + H_{0,0} M_{\mathbf{m},\mathbf{m}'} \end{aligned} \quad (7)$$

constitute the essential building blocks of CBF ground state theory. Together with the matrix elements of the density operator $\hat{\rho}(\mathbf{r})$

$$\rho_{\mathbf{m},\mathbf{m}'}(\mathbf{r}) \equiv \langle \Psi_{\mathbf{m}} | \hat{\rho}(\mathbf{r}) | \Psi_{\mathbf{m}'} \rangle \quad (8)$$

they are also key ingredients of our dynamic approach.

2.2. Boson dynamics

A natural generalization of the Jackson-Feenberg wave function to excited states is

$$|\Psi_t\rangle = \frac{1}{\sqrt{N_t}} e^{-\frac{i}{\hbar}t E_{\text{GS}}} F_{\text{GS}} e^{\frac{1}{2}\delta\hat{U}(t)} |\Phi_0\rangle , \quad (9)$$

where $|\Phi_0\rangle$ is unity for bosons. The fluctuation operator

$$\delta\hat{U}(t) = \sum_i \delta u^{(1)}(\mathbf{r}_i, t) + \sum_{i<j} \delta u^{(2)}(\mathbf{r}_i, \mathbf{r}_j, t) + \sum_{i<j<k} \delta u^{(3)}(\mathbf{r}_i, \mathbf{r}_j, \mathbf{r}_k, t) + \dots \quad (10)$$

is of a similar form as (4) but is now time dependent. Again, the $\delta u^{(n)}$ are determined by functional optimization, now based on the action principle corresponding to Schrödinger's equation.

Campbell *et al.*¹³ investigated ^4He , including fluctuations up to the pair level (*i.e.*, $n=2$). A recent study¹⁴ demonstrates i) that additional formal approximations to simplify the numerical treatment (the “uniform limit approximation” in Ref. 13) yield quite accurate results, and, ii) that pair fluctuations are highly relevant for correctly explaining large q dynamics. The state of the art for boson dynamics is to include triplet fluctuations,¹⁵ which correct the dynamic pair excitations in a self-consistent manner.

2.3. Fermion dynamics

The logical extension of the formalism to fermions is to express $\delta\hat{U}(t)$ of (10) by

$$\delta\hat{U}(t) = \sum_{\mathbf{p}_1 \mathbf{h}_1} \delta u_{\mathbf{p}_1 \mathbf{h}_1}^{(1)}(t) a_{\mathbf{p}_1}^\dagger a_{\mathbf{h}_1} + \frac{1}{2} \sum_{\mathbf{p}_1 \mathbf{h}_1 \mathbf{p}_2 \mathbf{h}_2} \delta u_{\mathbf{p}_1 \mathbf{h}_1 \mathbf{p}_2 \mathbf{h}_2}^{(2)}(t) a_{\mathbf{p}_1}^\dagger a_{\mathbf{h}_1} a_{\mathbf{p}_2}^\dagger a_{\mathbf{h}_2} + \dots \quad (11)$$

with \mathbf{p}_i and \mathbf{h}_i denoting states which are occupied and unoccupied in the ground state (“particles” and “holes”); spin-dependencies are not explicitly spelled out. The sheer increase in the number of variables ($\delta u^{(2)}$ depends on 4 vectors for fermions compared to 2 for bosons), prevents a solution on the same level of sophistication.

So-called “local approximations” assume that a quantity depends only on the momentum-transfer $\mathbf{q}_i = \mathbf{p}_i - \mathbf{h}_i$ of each particle-hole pair. If applied to the fluctuation amplitudes $\delta u^{(n)}$, the approach is of the same complexity as the bosonic theory. Though necessary for some quantities to obtain numerical tractability, making this simplification for a specific $\delta u^{(n)}$ squeezes the corresponding n -pair continuum into a single mode, and cannot give a proper explanation of the data in Fig. (1).

2.4. The cRPA

Omitting all $n \geq 2$ fluctuations for bosons yields the Bijl-Feynman spectrum,^{16,17} where the static structure factor $S(q)$ determines the collective mode dispersion

$$\chi^{\text{BF}}(q, \omega) = -\frac{\hbar^2 q^2 / m}{\omega^2 - \varepsilon_q^2} \quad \text{with} \quad \varepsilon_q \equiv \frac{\hbar^2 q^2}{2m S(q)}. \quad (12)$$

For fermions, not even the case $n=1$ can be solved analytically for χ . If exchange is neglected and the collective approximation is used for χ^0 (known as “plasmon pole approximation” in charged systems) the PH continuum shrinks into a single mode. This results again in the form (12). With the full particle-hole structure (but still neglecting exchange), Eq. (2), the cRPA, is obtained.⁶

For systems with a weak $v(q)$ the RPA is equivalent to time-dependent Hartree theory and the cRPA may also be interpreted as such, with an *effectively* weak interaction. Therefore our theory gives a systematic way to microscopically derive such interactions.^{18,19}

3. Fermion pair fluctuation theory

3.1. Linear response theory

For better clarity of the structure of the theory, we subsume the variables describing a particle-hole pair^a into a single number, $i \equiv (\mathbf{p}_i, \mathbf{h}_i)$. The system is subject to a weak external perturbation $h^{\text{ext}}(\mathbf{r}, t)$; this implies small deviations of the wave function from the ground state

$$|\Psi_t\rangle \approx |\Psi_{\text{GS}}\rangle + |\delta\Psi_t\rangle + \dots \quad (13)$$

^aIn $N_{\mathbf{m}, \mathbf{m}'}$ each index stands for *all* quantum numbers; *e.g.*, in the case of a single particle-hole excitation for $\mathbf{m} = (\mathbf{p}_1, \mathbf{h}_2, \dots, \mathbf{h}_N)$. Instead of spelling out the occupied states, we write $(\mathbf{p}_1, \mathbf{h}_1)$.

6 *H.M. Böhm, R. Holler, E. Krotscheck, M. Panholzer, H. Godfrin, M. Meschke, H.J. Lauter*

$\delta\Psi_t$ is obtained by expanding $\exp\{\delta\widehat{U}/2\}$ in (9) linearly in the fluctuations $\delta u^{(n)}$. This, in turn, gives the induced density $\delta\rho(\mathbf{r})$ as deviation from the ground state density ρ_{GS} in terms of CBF matrix elements:

$$\begin{aligned} \frac{1}{\mathcal{N}_t} \langle \Psi_t | \widehat{\rho}(\mathbf{r}) | \Psi_t \rangle &\approx \rho_{\text{GS}} + \delta\rho(\mathbf{r}) \\ \delta\rho(\mathbf{r}) &= \Re e \left\{ \sum_1 \delta u_1^{(1)} \delta\rho_{0,1}(\mathbf{r}) + \frac{1}{2} \sum_{1,2} \delta u_{12}^{(2)} \delta\rho_{0,12}(\mathbf{r}) \right\} \end{aligned} \quad (14)$$

(we suppress normalization factors $\sqrt{\mathcal{N}_{\mathbf{m}}/\mathcal{N}_0}$). The boson theory¹⁴ guides us to simplify (14) this by transforming to modified fluctuations defined as

$$\delta v(\mathbf{r}) \equiv \Re e \sum_1 \delta v_1^{(1)} \delta\rho_{0,1}(\mathbf{r}) . \quad (15)$$

Obviously, $\delta v^{(1)}$ implicitly sums two-pair correlations. The connection can be shown to involve the matrices of Eq. (7) via

$$\delta v_1^{(1)} = \delta u_1^{(1)} + \frac{1}{2} [M^{-1}]_{1,2} N_{2,34} \delta u_{43}^{(2)} , \quad (16)$$

(doubly appearing indices being summed). $N_{2,34}$ involves the states $(\mathbf{p}_2 \mathbf{h}_2, \mathbf{p}_3 \mathbf{h}_3, \mathbf{p}_4 \mathbf{h}_4)$ and thus 3-particle correlations. In the local approximation, this amounts to the (approximate) knowledge of the 3-particle ground state structure factor. The coefficient of $\delta u^{(2)}$ in (16) defines a new matrix

$$M_{1,23}^{\text{I}} \equiv (M^{-1} \cdot N)_{1,23} = [M^{-1}]_{1,4} N_{4,23} . \quad (17)$$

Diagrammatically, $M_{1,23}^{\text{I}}$ is a proper subset of $M_{1,23} = N_{1,23}$. Similarly, certain diagrams involving 4-particle correlations are canceled from $M_{12,34}$ by introducing

$$M_{12,34}^{\text{I}} \equiv (M + M^{\text{I}} \cdot M \cdot M^{\text{I}})_{12,34} \equiv M_{12,34} + M_{12,5}^{\text{I}} M_{5,6} M_{6,34}^{\text{I}} . \quad (18)$$

3.2. Equations of motion

Equations of motion (eom) follow straightforwardly from minimizing the action

$$\delta \int dt \frac{1}{\mathcal{N}_t} \langle \Psi_t | \widehat{H} + \widehat{H}^{\text{ext}} + \frac{\hbar}{i} \frac{\partial}{\partial t} | \Psi_t \rangle = 0 \quad ; \quad \widehat{H}^{\text{ext}} = \int d^3 r h^{\text{ext}}(\mathbf{r}, t) \widehat{\rho}(\mathbf{r}, t) \quad (19)$$

together with Eq. (13). Invoking the transformed fluctuation amplitude $\delta v^{(1)}$, the eom for the *two-pair* fluctuations $\delta u^{(2)}$ read

$$\begin{aligned} \frac{1}{2} \left[-M_{12,34}^{\text{I}} \frac{\hbar}{i} \frac{\partial}{\partial t} - K_{12,34} \right] \delta u_{43}^{(2)} &\equiv \frac{1}{2} \left[E_{12,34}(t) \right] \delta u_{43}^{(2)} \\ &= \frac{1}{2} K_{1234,0} \delta u_{43}^{(2)*} + K_{12,3} \delta v_3^{(1)} + K_{123,0} \delta v_3^{(1)*} . \end{aligned} \quad (20)$$

Here, the 4-pair coefficients are (written symbolically as well as explicitly)

$$\begin{aligned} K_{\mathbf{m},\mathbf{m}'} &\equiv \left[H' - (M^{\text{I}} \cdot H') - (H' \cdot M^{\text{I}}) + (H' \cdot M^{\text{I}} \cdot H') \right]_{\mathbf{m},\mathbf{m}'} , \\ K_{12,34} &\equiv H'_{12,34} - M_{12,5}^{\text{I}} H'_{5,34} - H'_{12,5} M_{5,34}^{\text{I}} + M_{12,5}^{\text{I}} H'_{5,6} M_{6,34}^{\text{I}} , \\ K_{1234,0} &\equiv H'_{1234,0} - M_{12,5}^{\text{I}} H'_{534,0} - H'_{125,0} M_{5,34}^{\text{I}} + M_{12,5}^{\text{I}} H'_{56,0} M_{6,34}^{\text{I}} , \end{aligned} \quad (21)$$

while the 3-pair coefficients take the simpler form

$$K_{\mathbf{m},\mathbf{m}'} \equiv \left[H' - (M^I \cdot H') \right]_{\mathbf{m},\mathbf{m}'} , \quad \begin{aligned} K_{12,3} &\equiv H'_{12,3} - M_{12,4}^I H'_{4,3} , \\ K_{123,0} &\equiv H'_{123,0} - M_{12,4}^I H'_{43,0} . \end{aligned} \quad (22)$$

Formally solving Eq. (20) yields $\delta u^{(2)}$ and $\delta u^{(2)*}$ as functions of the 1-pair fluctuations. These are then inserted into the eom for the 1-pair amplitudes:

$$\begin{aligned} \left[-M_{1,3} \frac{\hbar \partial}{i \partial t} - H'_{1,3} \right] \delta v_3^{(1)} - H'_{13,0} \delta v_3^{(1)*} &= 2 \int d^3 r \delta \rho_{1,0} h^{\text{ext}}(\mathbf{r}, t) \\ &+ \frac{1}{2} K_{1,34} \delta u_{43}^{(2)} + \frac{1}{2} K_{134,0} \delta u_{43}^{(2)*} . \end{aligned} \quad (23)$$

For practical purposes we neglect the static 4-body correlations $K_{1234,0} \approx 0$. Fourier transforming from time to frequency ω this implies for $u^{(2)}$

$$\begin{aligned} \frac{1}{2} \delta u^{(2)} &= [E^{-1}(\omega)] \cdot \left\{ K \cdot \delta v^{(1)} + K \cdot \delta v^{(1)*} \right\} , \\ \frac{1}{2} \delta u_{12}^{(2)} &= [E^{-1}(\omega)]_{12,56} \left\{ K_{65,3} \delta v_3^{(1)} + K_{653,0} \delta \delta v_3^{(1)*} \right\} . \end{aligned} \quad (24)$$

Inserting (24) on the r.h.s. of (23) gives an *effective single-particle equation*; therefore knowledge of the CBF matrices K and E^{-1} provides a 1:1 mapping onto *effective dynamic interactions*:

$$\begin{aligned} H'^{\text{eff}} \cdot \delta v^{(1)} &= H' \cdot \delta v^{(1)} + \frac{1}{2} K \cdot \delta u^{(2)} = \left[H' + K \cdot [E^{-1}(\omega)] \cdot K \right] \cdot \delta v^{(1)} \\ H'_{1,3}{}^{\text{eff}} \delta v_3^{(1)} &= H'_{1,3} \delta v_3^{(1)} + \frac{1}{2} K_{1,34} \delta u_{43}^{(2)} = \left[H'_{1,3} + K_{1,45} [E^{-1}(\omega)]_{54,67} K_{76,3} \right] \delta v_3^{(1)} \end{aligned} \quad (25)$$

(and the analogue for the $H'_{13,0}$ term).

4. Application of the theory

4.1. Approximations

How exchange effects correct the cRPA, was recently studied²⁰ for bulk ^3He ; their influence on multi-pair correlations is, presently, beyond numerical tractability within reasonable effort. We therefore decrease the number of variables by approximating $N_{\mathbf{m},\mathbf{m}'}$ and, consequently, M^I and K by their Fermi-sea average

$$N_{\mathbf{m},\mathbf{m}'} \rightarrow \frac{\sum_{\mathbf{h}_1 \dots \mathbf{h}_{m'}} N_{\mathbf{m},\mathbf{m}'}}{\sum_{\mathbf{h}_1 \dots \mathbf{h}_{m'}} n_{\mathbf{p}_1}^- n_{\mathbf{h}_1} \dots n_{\mathbf{p}_{m'}}^- n_{\mathbf{h}_{m'}}} . \quad (26)$$

Here, $n_{\mathbf{h}}$ denotes the Fermi distribution function and $n_{\mathbf{p}}^- \equiv 1 - n_{\mathbf{p}}$. The kinetic energy being intrinsically non-local, we split off the diagonal parts of the Hamiltonian:

$$H'_{\mathbf{m},\mathbf{m}'} \equiv W_{\mathbf{m},\mathbf{m}'} + \frac{1}{2} (H'_{\mathbf{m},\mathbf{m}} + H'_{\mathbf{m}',\mathbf{m}'}) N_{\mathbf{m},\mathbf{m}'} \quad (\mathbf{m} \neq \mathbf{m}') , \quad (27)$$

The $W_{\mathbf{m},\mathbf{m}'}$ can again be approximated locally by the procedure (26). The optimization of the ground state (3)-(4) ensures that the Fermi-sea average of $H'_{\mathbf{m},\mathbf{0}} = 0$, relating the local approximation of $W_{\mathbf{m},\mathbf{m}'}$ uniquely to that of $N_{\mathbf{m},\mathbf{m}'}$.

8 *H.M. Böhm, R. Holler, E. Krotscheck, M. Panholzer, H. Godfrin, M. Meschke, H.J. Lauter*

Denoting the Fourier transform of $\rho(\mathbf{r})$ with $\rho_{\mathbf{q}}$, the static structure factor $S(q)$ is expressed by its free value S_q^0 and CBF matrix elements via

$$S(q) = \frac{\langle \Psi_{\text{GS}} | \delta \hat{\rho}_{\mathbf{q}} \delta \hat{\rho}_{-\mathbf{q}} | \Psi_{\text{GS}} \rangle}{N \langle \Psi_{\text{GS}} | \Psi_{\text{GS}} \rangle} = S_q^0 + \frac{1}{N} \sum_{\mathbf{h} \neq \mathbf{h}'} N_{\mathbf{h}+\mathbf{q}, \mathbf{h}, \mathbf{h}'+\mathbf{q}} \quad (28)$$

This uniquely determines the local approximation of $N_{1,2}$. Similarly, $N_{1,2,3}$ is related to the 3-particle ground state structure factor, leading finally to

$$M_{1,2,3}^{\text{I}} \rightarrow \frac{S^{(3)}(\mathbf{q}_1, \mathbf{q}_2, \mathbf{q}_3)}{S(q_1) S_{q_2}^0 S_{q_3}^0} - \frac{S_{\mathbf{q}_1, \mathbf{q}_2, \mathbf{q}_3}^{(3)0}}{S_{q_1}^0 S_{q_2}^0 S_{q_3}^0} \quad (29)$$

Using the uniform limit approximation,¹³ $S^{(3)}$ factorizes this into products of $S(q_i)$. The 4-particle $M_{12,34}$ in (18) factorizes, too (neglecting terms of $\mathcal{O}(\frac{1}{N})$). Therefore, the only input for the dynamics is the ground state $S(q)$.

4.2. ^3He

In the experiment²¹ a mono layer of liquid ^3He was adsorbed on high quality exfoliated graphite, preplated by a mono layer of solid ^4He . The latter has the advantage of a weaker adsorption potential than the bare graphite; in addition, it smoothes out surface defects. At temperatures well below 1K the motion of the ^3He fluid is two-dimensional. It thus forms an atomically thick layer of known areal density. For the case reported here this is 4.9 atoms/nm².

On this layer we performed inelastic neutron scattering experiments at the Institut Laue Langevin (ILL) on the time-of-flight neutron spectrometer IN6. The accessible momentum transfers range from wave vectors $q = 2.54 \text{ nm}^{-1} \dots 20.46 \text{ nm}^{-1}$. The energy resolution is of the order of 0.1 meV.

For our calculations we use the $S(q)$ obtained from Fermi hypernetted chain theory^{12,22} as input. The results are shown in Fig. (2), for the same wave vectors and areal density as in the ILL experiment. Clearly, there is a large disagreement between the cRPA prediction (dashed lines) and the one including dynamic pair fluctuations (full lines), the spectra being *qualitatively* different. The dotted curves are obtained by convoluting the theoretical results with the experimental resolution of 0.1 meV and 1 nm^{-1} . This reproduces the main features of the experiment very well: a sharp mode above the PH continuum for q close to the Fermi momentum k_{F} (Fig. 2a), a very broad mode at intermediate q -values (Fig. 2b,c), and a resharpening of the mode at $3k_{\text{F}}$ (Fig. 2d).

The main effect of dynamic pair fluctuations is to shift strength towards lower energies; this is also true in the region of large Landau damping as is clearly seen in Fig. 2c. This type of qualitative change in $S(q, E)$ cannot be described by a static effective interaction. For the given areal density of 4.9 nm^{-2} the phonon-roton curve does not emerge from the PH band. However, for higher densities a maximum in $S(q, E)$ below the PH band is obtained, inaccessible to an RPA description.

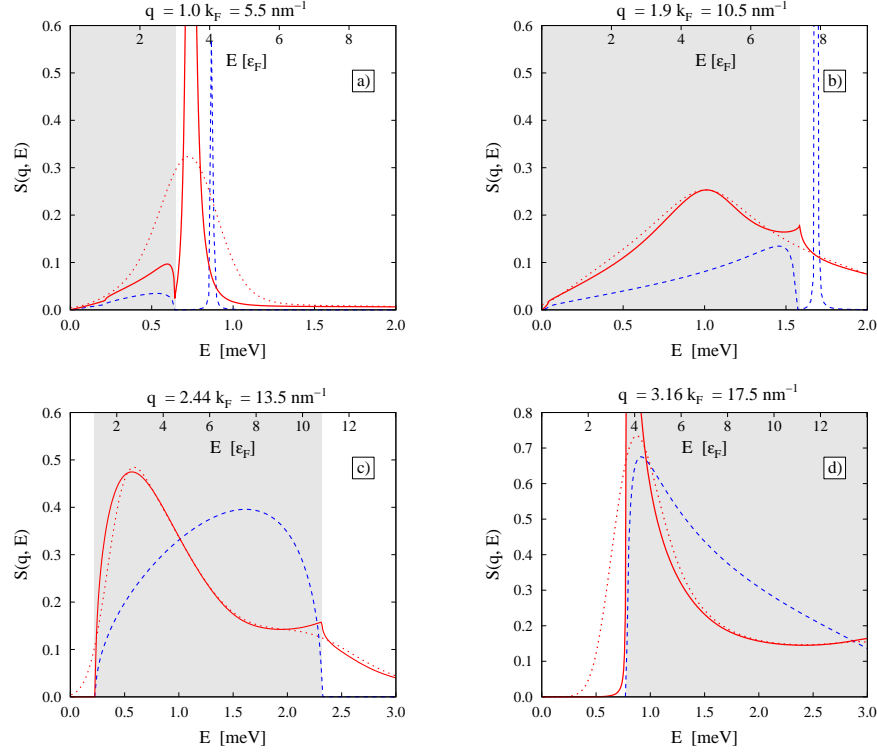


Fig. 2. (Color online) Comparison of the dynamic structure factor of ^3He , as obtained from the cRPA, Eq. (2), (dashed blue lines) and from the pair fluctuation theory (full red lines). The density and wave vectors q match those of Fig. 1. The dotted curves show the theoretical results convoluted with the experimental resolution.

4.3. Electron layers

For two-dimensional (2D) electrons the first prediction of a collective mode traversing the PH band was made by Neilson *et al.*²³ from quantum kinetic equations. Dynamic correlations were found important for density parameters^{2,3} r_s larger than 10. We here apply our theory to a 2D electron gas at $r_s=36$, close to Wigner crystallization. In analogy to ^3He we study the paramagnetic case.

For a 2D electron gas on graphite this means an areal density of the order of 10^{-1} nm^{-2} . Other realizations are electron layers in MOSFETS and/or semiconductor hetero-structures. In a GaAlAs-GaAs-GaAlAs quantum well, with a background dielectric constant $\epsilon_b = 12$ and an effective mass of 0.067 electron masses, the effective Bohr radius is roughly 100 \AA ; $r_s=36$ corresponds to $n \approx 10^{-2} \text{ nm}^{-2}$.

We obtained the input $S(q)$ for our calculations from Monte Carlo results by Gori-Giorgi *et al.*²⁴ Figure (3) shows that the effect of the dynamic pair fluctuations is the same as in ^3He : At small q the plasmon is sharp, though two-pair excitations cause a finite width while the cRPA plasmon is undamped. The one-pair excitations

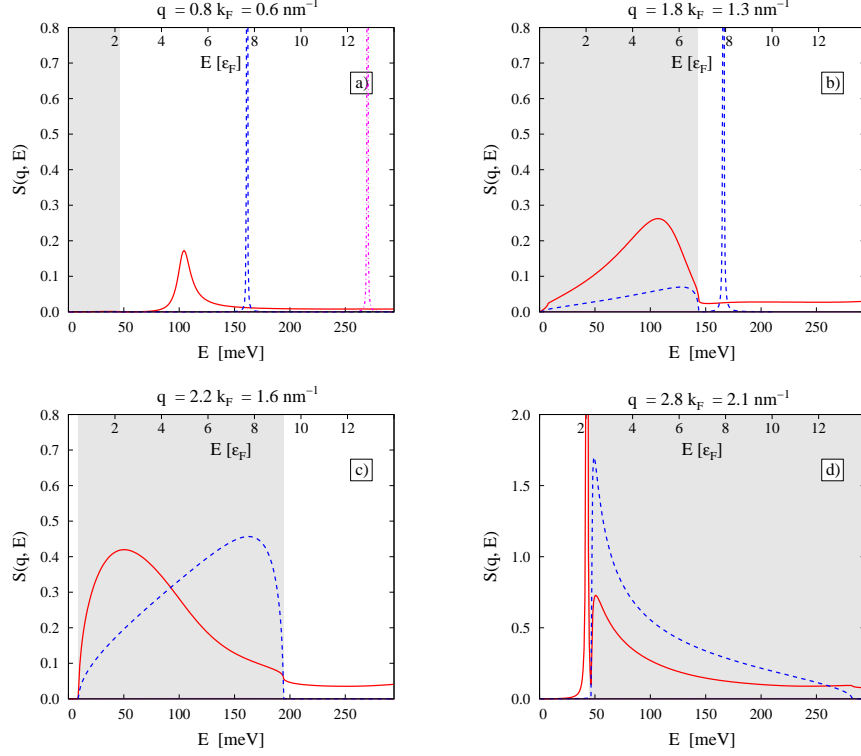
10 *H.M. Böhm, R. Holler, E. Krotscheck, M. Panholzer, H. Godfrin, M. Meschke, H.J. Lauter*

Fig. 3. (Color online) Comparison of the dynamic structure factor of a two-dimensional electron liquid at $r_s = 36$, in the cRPA, Eq. (2), (dashed blue lines) and from the pair fluctuation theory (full red lines). In the upper left graph also the bare RPA is seen (chained magenta line).

account for a large portion of the decrease of the dispersion in comparison to the bare RPA (Fig. 3a). In Fig. 3b, at intermediate q values, we find a broad and highly Landau-damped plasmon, in marked contrast with a sharp cRPA peak (the bare RPA plasmon is at a higher energy outside the range displayed). As in ^3He , with a further increase of q the spectrum “leans towards the left” (Fig. 3c) and, finally, resharpens on the lower side of the PH continuum in Fig. 3d. This recollection of strength is thus independent of the inter-particle interaction, the same effect arises for the long-ranged, soft-core Coulomb potential and the short-ranged, hard-core potential of helium. A close inspection of the data shows that the plasmon, indeed, re-emerges from the continuum, a feature that is beyond a cRPA approach with any effective static interaction.

5. Summary

We showed that variational dynamic quantum many body theory based on optimizing time-dependent fluctuation amplitudes provides a powerful tool for explaining the excitations of two-dimensional ^3He . For a full quantitative agreement with the

experimental results an inclusion of triplet fluctuations, exchange effects, or effective mass corrections may be required. The fermionic case being much more demanding than its bosonic counterpart, we concentrated our studies on the inclusion of two-pair fluctuations and could demonstrate that these give a major improvement over RPA-like approaches. The spectra obtained with pair fluctuations agree well with the scattering data on ^3He and qualitatively differ from any RPA result, both for helium and for electrons.

Our approach satisfies the ω^0 and ω^1 sum-rules and holds the potential for a systematic improvement. Aside from significantly changing the collective mode it also describes multi-pair damping and double-phonon / double-plasmon excitations.²⁵

Acknowledgements

This work was supported by the Austrian research fund FWF (project P21264) and under the Partenariat Hubert Curien “Amadeus”, as well as by the ILL neutron center and the EU FRP7 low temperature infrastructure (Grant 228464).

References

1. D. Pines, *Physics Today* **34**, 106 (Nov. 1981).
2. D. Pines and P. Nozieres, *The Theory of Quantum Liquids* (Benjamin, New York, 1966).
3. G. Giuliani and G. Vignale, *Quantum Theory of the Electron Liquid* (Cambridge University Press, Cambridge, 2005).
4. L. D. Landau, *Sov. Phys. JETP* **3**, p. 920 (1957).
5. H. Glyde, *Excitations in liquid and solid helium* (Oxford University Press, Oxford, 1994).
6. J. M. C. Chen, J. W. Clark and D. G. Sandler, *Z. Physik A* **305**, 223 (1982).
7. K. S. Singwi and M. P. Tosi, *Solid State Phys.* **36**, 177 (1981).
8. H. R. Glyde, B. Fåk, N. H. van Dijk, H. Godfrin, K. Guckelsberger and R. Scherm, *Phys. Rev. B* **61**, 1421 (2000).
9. M. M. Calbi and E. S. Hernández, *J. Low Temp. Phys.* **120**, 1 (2000).
10. J. Boronat, J. Casulleras, V. Grau, E. Krotscheck and J. Springer, *Phys. Rev. Lett.* **91**, 085302 (2003).
11. E. Feenberg, *Theory of Quantum Fluids* (Academic, New York, 1969).
12. E. Krotscheck, Theory of correlated basis functions, in *Introduction to Modern Methods of Quantum Many-Body Theory and their Applications*, eds. A. Fabrocini, S. Fantoni and E. Krotscheck, *Advances in Quantum Many-Body Theory*, Vol. 7 (World Scientific, Singapore, 2002) pp. 267–330.
13. C. C. Chang and C. E. Campbell, *Phys. Rev. B* **13**, 3779 (1976).
14. C. E. Campbell and E. Krotscheck, *Phys. Rev. B* **80**, 174501 (2009).
15. C. E. Campbell and E. Krotscheck, *to be published* (2010).
16. R. P. Feynman, *Phys. Rev.* **94**, 262 (1954).
17. A. Bijl, *Physica* **7**, 869 (1940).
18. E. Krotscheck and J. W. Clark, *Nucl. Phys. A* **328**, 73 (1979).
19. E. Krotscheck, *Phys. Rev. A* **26**, 3536 (1982).
20. M. Panholzer, H. M. Böhm, R. Holler and E. Krotscheck, *J. Low Temp. Phys.* **158**, 135 (2009).

- 12 *H.M. Böhm, R. Holler, E. Krotscheck, M. Panholzer, H. Godfrin, M. Meschke, H.J. Lauter*
21. H. Godfrin, M. Meschke, H. Lauter, H. M. Böhm, E. Krotscheck and M. Panholzer, *J. Low Temp. Phys.* **158**, 147 (2009).
22. E. Krotscheck, *J. Low Temp. Phys.* **119**, 103 (2000).
23. D. Neilson, L. Swierkowski, A. Sjölander and J. Szymanski, *Phys. Rev. B* **44**, 6291 (1991).
24. P. Gori-Giorgi, S. Moroni and G. Bachelet, *Phys. Rev. B* **70**, 115102/1 (2004).
25. H. M. Böhm, R. Holler, E. Krotscheck and M. Panholzer, *Int. J. Mod. Phys. B* **22**, 4655 (2008).